

Structural and Magnetic Properties Study of Gd³⁺/G-Cobalt Nanocomposite

G. Pavan Kumar ¹, Ch. Praveen Babu ¹, K. Radha Krishna ¹, A. Ramakrishna ^{2,3}, P. Padmavathi ¹, A. Mary Vijaya Ratna ¹, D. Parajuli ⁴, N. Murali ^{5,*} , K. Samatha ⁶

1 Department of Physics, St. Joseph's college for women (A), Visakhapatnam, A. P., India

2 Department of ECE, Aditya College of Engineering & Technology, Surampalem, India

3 Jawaharlal Nehru Technological University Kakinada, Kakinada, India

4 Research Center for Applied Science and Technology, Tribhuvan University, Kathmandu, Nepal

5 Department of Engineering Physics, AUCE (A), Andhra University, Visakhapatnam, Andhra Pradesh, India

6 Department of Physics, Andhra University, Visakhapatnam, Andhra Pradesh, India

* Correspondence: muraliphdau@gmail.com (N.M.);

Scopus Author ID 56151631900

Received: 9.08.2022; Accepted: 12.10.2022; Published: 24.12.2022

Abstract: The facile hydrothermal process was adopted to prepare Gd³⁺/G@CoFe₂O₄ magnetic material. The XRD, SEM, TEM, FTIR, and VSM were used for their structural, morphological, textural, functional group, and magnetic properties analysis. The samples were with pure spinel structure having lattice parameters increasing with increasing Gd³⁺ doped graphene. The 50-90 nm sized CoFe₂O₄ were spreading evenly over the Gd³⁺ doped graphene. FTIR shows cation stretching and vibrations within the 400–4000 cm⁻¹ wavenumber range. VSM shows the sample with magnetic nature which can be isolated from the solution using a simple magnet.

Keywords: Gd₃₊/G@CoFe₂O₄; ferrites; XRD; SEM; TEM; magnetic properties.

© 2021 by the authors. This article is an open-access article distributed under the terms and conditions of the Creative Commons Attribution (CC BY) license (<https://creativecommons.org/licenses/by/4.0/>).

1. Introduction

Materials with exotic physiochemical properties are not so easy to manufacture with the traditional methods [1-3]. The chemically stable and excellent magnetic materials like spinel ferrite (MFe₂O₄) are exploited today [4]. The wastes can be recycled by extracting spinel ferrites [5]. The magnetic cobalt ferrite (CoFe₂O₄) is useful in sensors, semiconductor catalysts activated under light, biomedicines, opto-magnetism, electrical, and antibacterial [6-10]. It has a bandgap of 2 eV, and an n-type semiconductor can be activated by normal light [11]. Their controlled morphology can contribute to their physicochemical properties [12-15]. Gd³⁺ doped graphene has enormous conductivity [16]. The trivalent ions substitution in the octahedral site was studied extensively [17-20]. The preparation methods like sol-gel, hydrothermal, coprecipitation, etc., greatly affect the properties of the prepared samples [21-25]. Commercially viable ferrites can be obtained from a simple and controlled preparation [26].

This paper adopted the hydrothermal method to prepare Gd³⁺/graphene substituted cobalt ferrite and characterized with XRD, SEM, TEM, FTIR, and VSM for their respective properties.

2. Materials and Methods

Phosphoric acid, sulfuric acid, ethanol were bought from Thomas baker and iron acetate, cobalt acetate, gadolinium nitrate, potassium permanganate, potassium hydroxide and Vulcan carbon were bought from Sigma-Aldrich.

2.1. Synthesis reduced graphene oxide (RGO) and Gd^{3+}/G

The flake of graphite powder was used for the preparation of RGO with the help of Hummer's method [36], which further gives Gd^{3+} -doped graphene (NG). In this method, 60 mL RGO solution was ultrasonicated in a round bottom flask for half an hour and added 0.5 g of urea onto it. The solution is then transferred to a Teflon-lined autoclave under 180 °C for 24 h, filtered NG. The resultant was then washed with alcohol and double distilled water. It was finally dried at 80 °C for 12 h.

2.2. Synthesis of $Gd^{3+}/G @ CoFe_2O_4$

50 mg of Gd^{3+}/G was mixed with 15 mL of distilled water. The resultant was mixed with a 50 mg acetate mixture of iron and cobalt in the molar ratio of 2:1. It was washed with ethanol and stirred at room temperature for 24 h to combine Co^{2+} and Fe^{2+} ions with Gd^{3+} nitrate and oxy functional groups on the graphene framework. The resultant is transferred into a 50 mL Teflon-lined stainless steel autoclave maintained at 120 °C for 12 h. Filtration of the solution and drying at 60 °C give $Gd^{3+}/G @ CoFe_2O_4$. Similarly, $CoFe_2O_4$ was synthesized.

3. Results and Discussion

3.1. XRD Study

A powered X-ray diffractometer (XRD) was used to determine the structural parameters of RGO, Gd^{3+}/G , $CoFe_2O_4$, and $Gd^{3+}/G @ CoFe_2O_4$, whose patterns are shown in Figure 1 (a) and (b). RGO and Gd^{3+}/G correspond to the peak ($2\theta^\circ$) at 24.9° (002) and 24.3° (002), respectively, and agree with JCPDS Card No. 75-1621 [27]. The diffraction peaks in Fig. 1 (c) and (d) are related to the $CoFe_2O_4$ and $CoFe_2O_4 @ Gd^{3+}/G$ nanocomposite matching with JCPDS No. 00-022-1086 [28]. The (002) diffraction peak becomes weaker due to the destruction of the stacking of interlayer cobalt ferrite nanorods [29]. However, $CoFe_2O_4$ and $CoFe_2O_4 @ Gd^{3+}/G$ nanocomposites have intense peaks indicating their good crystallinity nature.

The lattice constant and average crystallite size is found with Bragg's law [30] and the Debye Sherer formula [31].:

$$a = d\sqrt{h^2 + k^2 + l^2} \tag{1}$$

$$D_{311} = \frac{0.9\lambda}{\beta \cos\theta} \tag{2}$$

Where d is the interplanar spacing and h, k, l are the miller indices. λ , β , and θ are the wavelength of X-ray, FWHM of (311) peak, and diffracting angle, respectively.

The synthesized nanoparticles' lattice constant and crystallite size values were 8.423 Å and 8.428 Å between 25 nm and 40 nm, as shown in Table 1. The synthesized ferrites' nanostructured materials are confirmed by the XRD crystalline calculation [32].

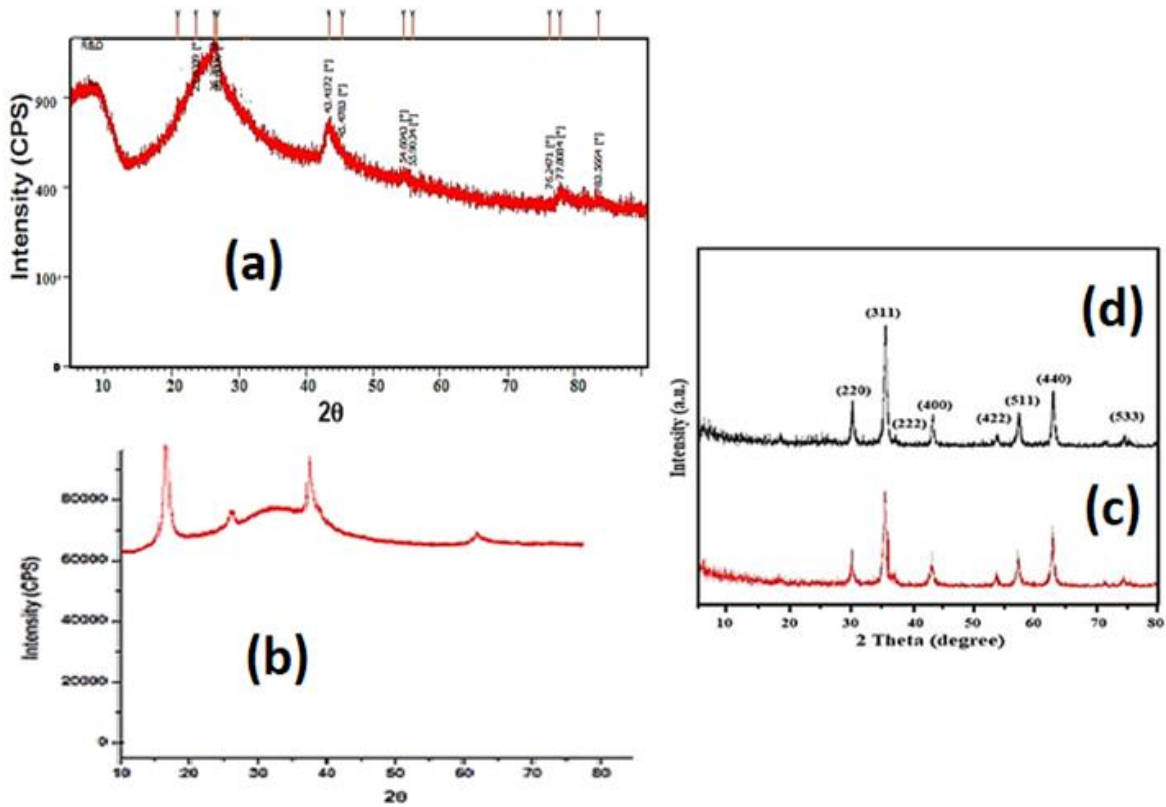


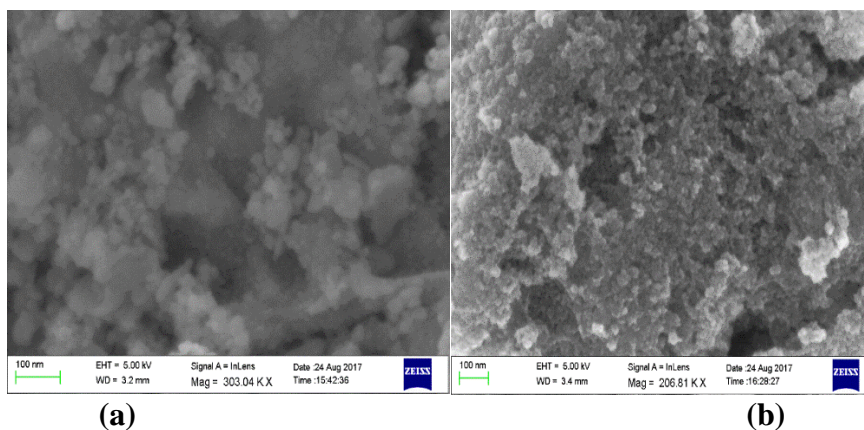
Figure 1. PXRD pattern of (a) RGO and (b) NG (c) CoFe₂O₄ and (d) Gd³⁺/G@CoFe₂O₄.

Table 1. Crystallite size value of CoFe₂O₄ and CoFe₂O₄ @Gd³⁺/G nanoparticles.

Composition (x)	Lattice constant (Å)	Crystallite size (nm)	Space group
CoFe ₂ O ₄	8.423	25	Fd-3m
CoFe ₂ O ₄ @Gd ³⁺ /G	8.428	40	Fd-3m

3.2. Scanning and transmission electron microscopy studies.

The SEM images of the (a) RGO and (b) NG, (c) CoFe₂O₄, and (d) Gd³⁺/G@CoFe₂O₄ are shown in Figure 2 (a) to (d), where the nanorods of cobalt ferrites and the cobalt ferrites nanorods in Gd³⁺/G are seen clearly. The estimated particle size values were determined from this study to be in the range of 50 nm to 90 nm. The agglomeration of the particle collections caused an inhomogeneous size distribution after the low-temperature sintering processes, which caused the size variation [33]. Similarly, the respective TEM images of GO, Gd³⁺/G, CoFe₂O₄, and Gd³⁺/G @ CoFe₂O₄ in Figure 3 (a) to (d). The GO has lamellar, and Gd³⁺/G has a dense texture. The layered Gd³⁺/G show the incorporation and agglomeration of CoFe₂O₄ nanotubes.



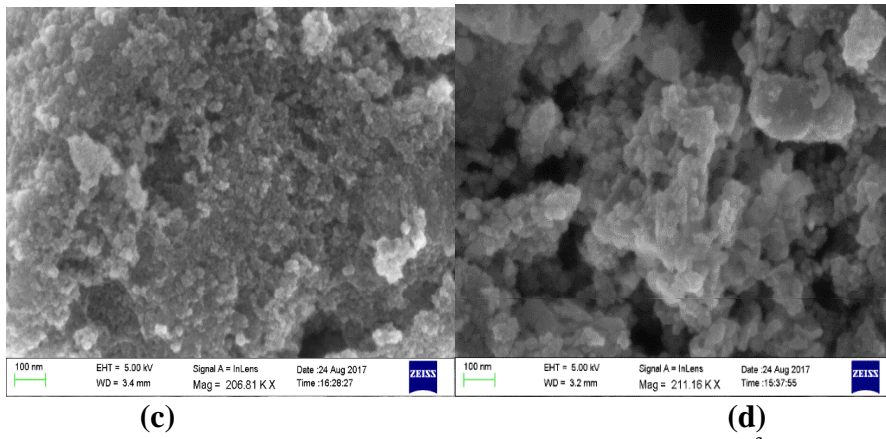


Figure 2. SEM micrographs of (a) GO, (b) NG, (c) CoFe₂O₄ and (d) Gd³⁺/G@CoFe₂O₄.

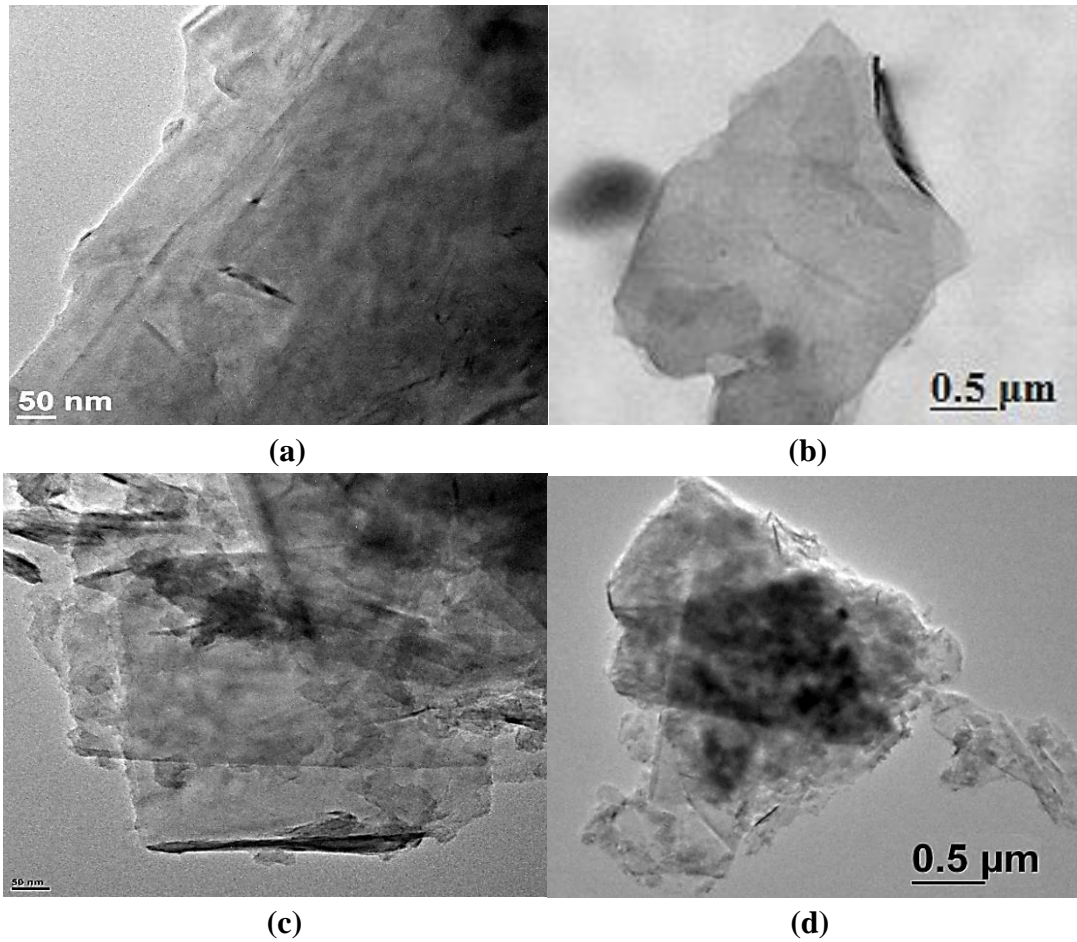


Figure 3. TEM micrographs of (a) GO, (b) NG, (c) CoFe₂O₄ and (d) Gd³⁺/G@CoFe₂O₄.

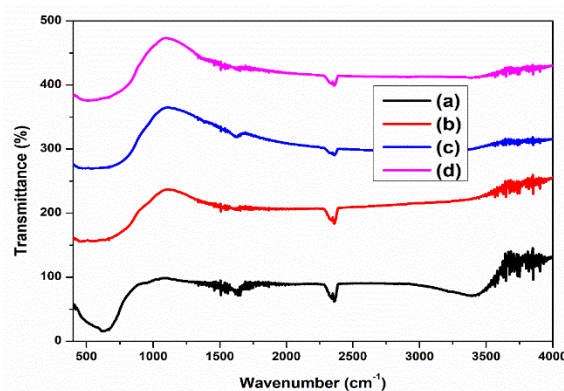


Figure 3. FTIR spectrum of (a) GO, (b) NG, (c) CoFe₂O₄ and (d) Gd³⁺/G@CoFe₂O₄.

3.3. FTIR studies.

Figure 3 shows the FTIR spectra of (a) GO, (b) NG, (c) CoFe₂O₄ and (d) Gd³⁺/G@CoFe₂O₄. The vibration due to stretching of carbonyl, aromatic, carboxylic, epoxy, and alkoxy (with the respective notations O-H, C=O, C=C, C-OH, C-O, and C-O) giving a peak at around 3353, 1730, 1621, 1386, 1239, 1082 and 1032 cm⁻¹ respectively. However, the functional group related to oxygen that is not visible in Gd³⁺ doped graphene might be of the synthesis process and doping. The peaks around 1568 and 1212 cm⁻¹ are due to the sheets of graphene. Their frequency is shifted towards red in the spectrum of Gd³⁺/G @CoFe₂O₄ related to the graphene sheet, which might be due to the insertion of cobalt ferrite in the framework of Gd³⁺/G as shown in Figure 4. The peak around 589 cm⁻¹ is due to Fe-O, indicating the presence of CoFe₂O₄ [34]. Due to the distance variation between Fe³⁺ and O²⁻ ions from the given figure, there is a small shift to the higher wavenumbers caused by substitution content [35].

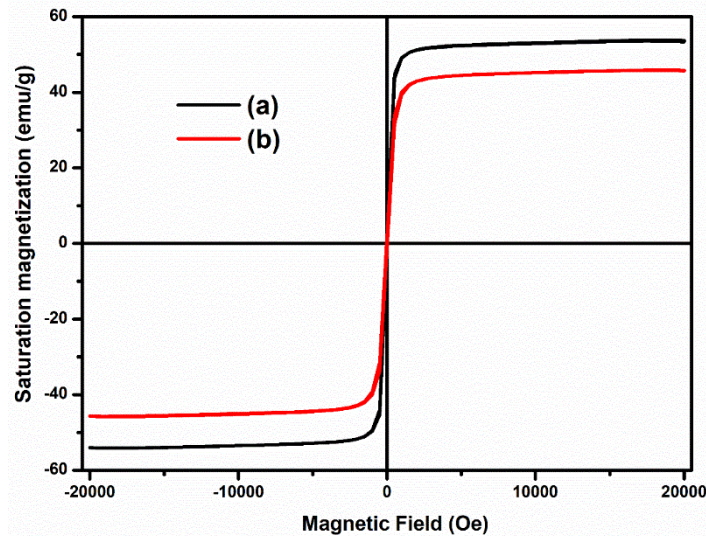


Figure 4. Magnetic hysteresis loop of (a) CoFe₂O₄ and (b) Gd³⁺/G@CoFe₂O₄.

3.4. Magnetic properties.

The hysteresis loops obtained from the VSM analysis reveal the sample's highly magnetic characteristics (like M_s, M_r, H_c, R, K, μB), as shown in Figure 4. The saturation magnetization/coercivity is 53.73/45.84 emu/g, and 1105.32/480.21Oe are found for CoFe₂O₄ and Gd³⁺/G@CoFe₂O₄. The non-magnetic nature of Gd³⁺/G reduces the magnetic saturation value of Gd³⁺/G@CoFe₂O₄. However, adding magnetic material with Gd³⁺/G may tune the magnetic behavior significantly, as mentioned in the previous literature [36].

The formula is used to calculate the remnant ratio [37].

$$R = \frac{M_r}{M_s} \tag{3}$$

The application of prepared ferrites is shown by the remnant ratio. A ratio value smaller than 1 indicates that the materials are suitable for sensitivity applications [38]. However, it is seen that the value increases as the concentration of the dopant increases, suggesting that doped samples are also suitable for memory storage devices.

The magnetic moment is determined using the formula below [39].

$$\mu_B = M \times \frac{M_s}{5585} \tag{4}$$

where M is the measured sample's molecular weight.

It has been found that magnetic moment increases as doping concentrations increase. However, all the results remained relatively stable, indicating that all the samples exhibited minimal energy losses [40].

Additionally, the following formula is used to calculate the anisotropy constant [41].

$$K = \frac{H_c \times M_s}{0.96} \quad (3)$$

Due to an increase in saturation magnetization and a considerable decrease in coercivity. The doping concentration is inversely related to magnetic anisotropy. This shows how the synthesized doping samples increase the magnetic crystallinity in ferrite samples [42]. The magnetic parameters of synthesized sample values are shown in table 2.

Table 2. Magnetic parameters of CoFe₂O₄ and CoFe₂O₄ @Gd³⁺/G nanoparticles.

Concentration (x)	M _s (emu/g)	H _c (Oe)	M _r (emu/g)	M _r /M _s (emu/g)	Magnetic moment μB	Anisotropy constant (erg/g)
CoFe ₂ O ₄	54.26	325	30.51	0.56	2.12	19.268
CoFe ₂ O ₄ @Gd ³⁺ /G	45.15	264	28.54	0.63	2.05	12.565

4. Conclusions

The hydrothermal process successfully prepared CoFe₂O₄ and Gd³⁺/G@CoFe₂O₄ nanocomposites and characterized their structural, morphological, textural, functional, and magnetic properties. Gd³⁺/G@CoFe₂O₄ is separated with a simple bar magnet. Powder XRD show Gd³⁺/G@CoFe₂O₄ nanocomposites in the framework of cubic spinel cobalt ferrite. The average crystallite was found in the range of 50-90 nm. The addition of non-magnetic Gd³⁺/G reduces, and the suitable addition of CoFe₂O₄ increases the saturation magnetization of the Gd³⁺/G@CoFe₂O₄ nanocomposites.

Funding

The authors are thankful to the researchers supporting the program at St. Joseph's college for women (A) for the financial support through the minor project.

Acknowledgments

We would like to thank St. Joseph's college for women (A), Visakhapatnam, for its continued support of our research.

Conflicts of Interest

We declare that this article has no conflict of interest.

References

1. Yonatan Mulushoa, S.; Tulu Wegayehu, M.; Tewodros Aregai, G.; Murali N.; Sushma Reddi, M.; Vikram Babu, B.; Arunamani, T.; Samatha K. Synthesis of spinel MgFe₂O₄ ferrite material and studying its structural and morphological properties using solid state method. *Chem Sci Trans.* **2017**, *6*, 653-661, <https://doi.org/10.7598/cst2017.1401>.
2. Mulushoa, S.Y.; Kumari, C.V.; Raghavendra, V.; Babu, K.E.; Murthy, B.S.N.; Suribabu, K.; Ramakrishna, Y.; Murali, N. Effect of Zn–Cr substitution on the structural, magnetic and electrical properties of magnesium ferrite materials. *Physica B: Condensed Matter* **2019**, *572*, 139-147, <https://doi.org/10.1016/j.physb.2019.07.057>.

3. Himakar, P.; Jayadev, K. Parajuli, D.; Murali, N.; Taddesse, P.; Mulushoa, S.Y.; Mammo, T.W.; Kishore Babu, B.; Veeraiah, V.; Samatha, K. Effect of Cu substitution on the structural, magnetic, and dc electrical resistivity response of $\text{Co}_{0.5}\text{Mg}_{0.5-x}\text{Cu}_x\text{Fe}_2\text{O}_4$ nanoferrites. *Applied Physics A* **2021**, *127*, 371, <https://doi.org/10.1007/s00339-021-04521-w>.
4. Chandramouli, K.; Suryanarayana, B.; Phanidhar Varma, P.V.S.K.; Raghavendra, V.; Emmanuel, K.A.; Taddesse, P.; Murali, N.; Wegayehu Mammo, T.; Parajuli, D. Effect of Cr^{3+} substitution on dc electrical resistivity and magnetic properties of $\text{Cu}_{0.7}\text{Co}_{0.3}\text{Fe}_{2-x}\text{Cr}_x\text{O}_4$ ferrite nanoparticles prepared by sol-gel auto combustion method. *Results in Physics* **2021**, *24*, 104117, <https://doi.org/10.1016/j.rinp.2021.104117>.
5. Chandramouli, K.; Rao, P.A.; Suryanarayana, B.; Raghavendra, V.; Mercy, S.J.; Parajuli, D.; Taddesse, P.; Mulushoa, S.Y.; Mammo, T.W.; Murali, N. Effect of Cu substitution on magnetic and DC electrical resistivity properties of Ni–Zn nanoferrites. *Journal of Materials Science: Materials in Electronics* **2021**, *32*, 15754-15762, <https://doi.org/10.1007/s10854-021-06127-7>.
6. Anantha Rao, P.; Raghavendra, V.; Suryanarayana, B.; Paulos, T.; Murali, N.; Phanidhar Varma, P.V.S.K.; Giri Prasad, R.; Ramakrishna, Y.; Chandramouli, K. Cadmium substitution effect on structural, electrical and magnetic properties of Ni-Zn nano ferrites. *Results in Physics* **2020**, *19*, 103487, <https://doi.org/10.1016/j.rinp.2020.103487>.
7. Jesus Mercy, S.; Parajuli, D.; Murali, N.; Ramakrishna, A.; Ramakrishna, Y.; Veeraiah, V.; Samatha, K. Microstructural, thermal, electrical and magnetic analysis of Mg^{2+} substituted Cobalt ferrite. *Applied Physics A* **2020**, *126*, 873, <https://doi.org/10.1007/s00339-020-04048-6>.
8. Suryanarayana, B.; Ramanjaneyulu, K.; Raghavendra, V.; Murali, N.; Parajuli, D.; Mulushoa, S.Y.; Choppa, P.; Rao, P.A.; Ramakrishna, Y.; Chandramouli, K. Effect of Sm^{3+} substitution on dc electrical resistivity and magnetic properties of Ni–Co ferrites. *Journal of the Indian Chemical Society* **2022**, *99*, 100623, <https://doi.org/10.1016/j.jics.2022.100623>.
9. Daruvuri, H.R.; Chandu, K.; Murali, N.; Parajuli, D.; Dasari, M.P. Effect on structural, dc electrical resistivity, and magnetic properties by the substitution of Zn^{2+} on Co-Cu nano ferrite. *Inorganic Chemistry Communications* **2022**, *143*, 109794, <https://doi.org/10.1016/j.inoche.2022.109794>.
10. Mammo, T.W.; Murali, N.; Kumari, C.V.; Margarete, S.J.; Ramakrishna, A.; Vemuri, R.; Shankar Rao, Y.B.; Vijaya Prasad, K.L.; Ramakrishna, Y.; Samatha, K. Synthesis, structural, dielectric and magnetic properties of cobalt ferrite nanomaterial prepared by sol-gel autocombustion technique. *Physica B: Condensed Matter* **2020**, *581*, 411769, 164-170, <https://doi.org/10.1016/j.physb.2017.12.049>.
11. Chandra Babu Naidu K.; RoopasKiran S.; Madhuri W. Investigations on transport, impedance and electromagnetic interference shielding properties of microwave processed NiMg ferrites. *Materials Research Bulletin* **2017**, *89*, 125-138, <https://doi.org/10.1016/j.materresbull.2017.01.015>.
12. Naidu, K.C.B.; Kiran, S.R.; Madhuri, W. Microwave processed NiMgZn ferrites for electromagnetic interference shielding applications. *IEEE Transactions on Magnetics* **2016**, *53*, 1-7, <https://doi.org/10.1109/TMAG.2016.2625773>.
13. Raghuram, N.; Rao, T.S.; Naidu, K.C.B. Electrical and impedance spectroscopy properties of hydrothermally synthesized $\text{Ba}_{0.2}\text{Sr}_{0.8-y}\text{La}_y\text{Fe}_{12}\text{O}_{19}$ ($y = 0.2-0.8$) nanorods. *Ceramics International* **2020**, *46*, 5894-5906, <https://doi.org/10.1016/j.ceramint.2019.11.042>.
14. Naidu, K.C.B.; Wuppuluri, M. Ceramic nanoparticle synthesis at lower temperatures for LTCC and MMIC technologies. *IEEE Transactions on Magnetics* **2018**, *54*, 1-8, <https://doi.org/10.1109/TMAG.2018.2855663>.
15. Kumar, D.S.; Naidu, K.C.B.; Rafi, M.M.; Nazeer, K.P.; Begam, A.A.; Kumar, G.R. Structural and dielectric properties of superparamagnetic iron oxide nanoparticles (SPIONs) stabilized by sugar solutions. *Mater Sci Pol.* **2018**, *36*, 123-133, <https://doi.org/10.1515/msp-2018-0017>.
16. Chandra Babu Naidu, K.; Madhuri, W. Effect of Nonmagnetic Zn^{2+} Cations on Initial Permeability of Microwave-Treated NiMg Ferrites. *International Journal of Applied Ceramic Technology* **2016**, *13*, 1090-1095, <https://doi.org/10.1111/ijac.12571>.
17. Sagar, T.V.; Rao, T.S.; Naidu, K.C.B. Effect of calcination temperature on optical, magnetic and dielectric properties of Sol-Gel synthesized $\text{Ni}_{0.2}\text{Mg}_{0.8-x}\text{Zn}_x\text{Fe}_2\text{O}_4$ ($x = 0.0-0.8$). *Ceramics International* **2020**, *46*, 11515-11529, <https://doi.org/10.1016/j.ceramint.2020.01.178>.
18. Raghuram, N.; Rao, T.S.; Naidu, K. Magnetic properties of hydrothermally synthesized $\text{Ba}_{1-x}\text{Sr}_x\text{Fe}_{12}\text{O}_{19}$ ($x = 0.0-0.8$) nanomaterials. *Applied Physics A*. **2019**, *125*, 1-15, <https://doi.org/10.1007/s00339-019-3143-2>.
19. Sivakumar, D.; Chandra Babu Naidu, K.; Prem Nazeer. K.; Mohamed Rafi. M.; Ramesh kumar. G.; Sathyaseelan. B.; Killivalavan. G.; Ayisha Begam. A. Structural Characterization and Dielectric Studies of

- Superparamagnetic Iron Oxide Nanoparticles. *Journal of the Korean Ceramic Society* **2018**, *55*, 230-238, <https://doi.org/10.4191/kcers.2018.55.3.02>.
20. Kadiyala, C.B.N.; and Wuppulluri, M. Effect of microwave heat treatment on pure phase formation of hydrothermal synthesized nano NiMg ferrites. *Phase Transitions* **2017**, *90*, 847-862, <https://doi.org/10.1080/01411594.2016.1277220>.
 21. Alhashmialameer, D.; Ullah, S.; Irshad, A.; Alsafari, I.A.; Abd El-Gawad, H.H.; Elsheikh, M.A.A.; Liu, X.; Bashir, S. Copper-doped magnesium ferrite and its composite with rGO: Synthesis, characterization, and degradation of organic effluents and antibacterial study. *Ceramics International* **2022**, *48*, 24100-24113, <https://doi.org/10.1016/j.ceramint.2022.05.373>.
 22. Kumar, S.R.; Priya, G.V.; Aruna, B.; Raju, M.K.; Parajuli, D.; Murali, N.; Verma, R.; Batoo, K.M.; Kumar, R.; Narayana, P.L. Influence of Nd³⁺ substituted Co_{0.5}Ni_{0.5}Fe₂O₄ ferrite on structural, morphological, dc electrical resistivity and magnetic properties. *Inorganic Chemistry Communications* **2022**, *136*, 109132, <https://doi.org/10.1016/j.inoche.2021.109132>.
 23. Hssaini, A.; Belaiche, M.; Elansary, M.; Ferdi, C.A.; Mouhib, Y. Magnetic and Structural Properties of Novel-Coated Ni_{0.5}Co_{0.5}Fe_{1.6}Gd_{0.2}Mo_{0.1}Sm_{0.1}O₄ Spinel Ferrite Nanomaterial: Experimental and Theoretical Investigations. *Journal of Superconductivity and Novel Magnetism* **2022**, 1-22, <https://doi.org/10.1007/s10948-022-06307-4>.
 24. Jafarpour, M.; Rostami, M.; Khalkhali, S.M.H.; Nikmanesh, H.; Ara, M.H.M. The effect of lanthanum substitution on the structural, magnetic, and dielectric properties of nanocrystalline Mn-Ni spinel ferrite for radio frequency (RF) applications. *Physics Letters A* **2022**, *446*, 128285, <https://doi.org/10.1016/j.physleta.2022.128285>.
 25. Bashir, S.; Jamil, A.; Amin, R.; Ul-hasan, I.; Alazmi, A.; Shahid, M. Hydrothermally synthesized Gd-doped BiSbO₄ nanoparticles and their graphene-based composite: A novel photocatalytic material. *Journal of Solid State Chemistry* **2022**, *312*, 123217, <https://doi.org/10.1016/j.jssc.2022.123217>.
 26. Akhtar, M.N.; Yousaf, M.; Lu, Y.; Mahmoud, M.Z.; Iqbal, J.; Khan, M.A.; Khallidoon, M.U.; Ullah, S.; Hussien, M. Magnetic, structural, optical band alignment and conductive analysis of graphene-based REs (Yb, Gd, and Sm) doped NiFe₂O₄ nanocomposites for emerging technological applications. *Synthetic Metals* **2022**, *284*, 116994, <https://doi.org/10.1016/j.synthmet.2021.116994>.
 27. Wani, T.A.; Suresh, G. Plant Mediated Green Synthesis of Magnetic Spinel Ferrite Nanoparticles: A Sustainable Trend in Nanotechnology. *Advanced Sustainable Systems* **2022**, 2200035. <https://doi.org/10.1002/adsu.202200035>.
 28. Morais, P.V.; Orlandi, M.O.; Schöning, M.J.; Siqueira Jr, J.R. Layer-by-Layer Films with CoFe₂O₄ Nanocrystals and Graphene Oxide as a Sensitive Interface in Capacitive Field-Effect Devices. *ACS Applied Nano Materials* **2022**, *5*, 5258-5267, <https://doi.org/10.1021/acsanm.2c00296>.
 29. Kırak, B.; Tümen, K.U.; Karaaslan, M.; Akyol, M. Investigation of structural, magnetic and microwave absorption properties of Ni_xCo_{1-x}Fe₂O₄/Ni: ZnO (x: 0.0, 0.5, and 1.0) embedded epoxy composites. *Applied Physics A* **2022**, *128*, 1-8. <https://doi.org/10.1007/s00339-022-05905-2>.
 30. Du, R.; Cao, H.; Wang, G.; Dou, K.; Tsidaeva, N.; Wang, W. PVP modified rGO/CoFe₂O₄ magnetic adsorbents with a unique sandwich structure and superior adsorption performance for anionic and cationic dyes. *Separation and Purification Technology* **2022**, *286*, 120484, <https://doi.org/10.1016/j.seppur.2022.120484>.
 31. Priya, G.V.; Murali, N.; Raju, M.K.; Krishan, B.; Parajuli, D.; Choppara, P.; Sekhar, B.C.; Verma, R.; Batoo, K.M.; Narayana, P.V. Influence of Cr³⁺ substituted NiZnCo nano-ferrites: structural, magnetic and DC electrical resistivity properties. *Applied Physics A* **2022**, *128*, 1-8, <https://doi.org/10.1007/s00339-022-05809-1>.
 32. Parajuli, D.; Murali, N.; Rao, A.V.; Ramakrishna, A.; Samatha, K. Structural, dc electrical resistivity and magnetic investigation of Mg, Ni, and Zn substituted Co-Cu nano spinel ferrites. *South African Journal of Chemical Engineering* **2022**, *42*, 106-114, <https://doi.org/10.1016/j.sajce.2022.07.009>.
Naidu, K.C.B.; Sarmash, T.S.; Reddy, V.N.; Maddaiah, M.; Reddy, P.S. and Subbarao, T. Structural, dielectric and electrical properties of La₂O₃ doped SrTiO₃ ceramics. *Journal of The Australian Ceramic Society* **2015**, *51*, 94-102.
 33. Chandra Babu Naidu, K.; Narasimha Reddy, V.; Sofi Sarmash, T.; Kothandan, D.; Subbarao, T.; Suresh Kumar, N. Structural, morphological, electrical, impedance and ferroelectric properties of BaO-ZnO-TiO₂ ternary system. *Journal of the Australian Ceramic Society* **2019**, *55*, 201-218, <https://doi.org/10.1007/s41779-018-0225-0>.

34. Kumar, N.S.; Suvarna, R.P.; Naidu, K.C.B. Microwave heated lead cobalt titanate nanoparticles synthesized by sol-gel technique: structural, morphological, dielectric, impedance and ferroelectric properties. *Materials Science and Engineering: B* **2019**, *242*, 23-30. <https://doi.org/10.1016/j.mseb.2019.03.005>.
35. Mulushoa, S.Y.; Kumari, C.V.; Raghavendra, V.; Babu, K.E.; Murthy, B.S.N.; Suribabu, K.; Ramakrishna, Y.; and Murali, N. Effect of Zn–Cr substitution on the structural, magnetic and electrical properties of magnesium ferrite materials. *Physica B: Condensed Matter* **2019**, *572*, 139-147, <https://doi.org/10.1016/j.physb.2019.07.057>.
36. Kumar, N.S.; Suvarna, R.P.; Naidu, K.C.B. Multiferroic Nature of Microwave-Processed and Sol-Gel Synthesized Nano $Pb_{1-x}Co_xTiO_3$ ($x= 0.2-0.8$) Ceramics. *Crystal Research and Technology* **2018**, *53*, 1800139, <https://doi.org/10.1002/crat.201800139>.
37. Parajuli, D.; Tadesse, P.; Murali, N.; Samatha, K. Correlation between the structural, magnetic, and dc resistivity properties of $Co_{0.5}M_{0.5-x}Cu_xFe_2O_4$ ($M= Mg, \text{ and } Zn$) nano ferrites. *Applied Physics A* **2022**, *128*, 1-9, <https://doi.org/10.1007/s00339-021-05211-3>.
38. Kothandan, D.; Jeevan Kumar, R. and Chandra Babu Naidu, K. Barium titanate microspheres by low temperature hydrothermal method: studies on structural, morphological, and optical properties. *Journal of Asian Ceramic Societies* **2018**, *6*, 1-6, <https://doi.org/10.1080/21870764.2018.1439607>.
39. Dastagiri, S.; Lakshmaiah, M.V.; Chandra Babu Naidu, K.; Suresh Kumar, N. and Khan, A. Induced dielectric behavior in high dense $Al_xLa_{1-x}TiO_3$ ($x= 0.2-0.8$) nanospheres. *Journal of Materials Science: Materials in Electronics* **2019**, *30*, 20253-20264, <https://doi.org/10.1007/s10854-019-02409-3>.
40. Himakar, P.; Jayadev, K.; Parajuli, D.; Murali, N.; Tadesse, P.; Mulushoa, S.Y.; Mammo, T.W.; Kishore Babu, B.; Veeraiah, V. and Samatha, K.. Effect of Cu substitution on the structural, magnetic, and dc electrical resistivity response of $Co_{0.5}Mg_{0.5-x}Cu_xFe_2O_4$ nanoferrites. *Applied Physics A* **2021**, *127*, pp.1-10. <https://doi.org/10.1007/s00339-021-04521-w>.
41. Geetha, P.; Tadesse, P.; Murali, N.; Narayana, P.L. Impact of Gd^{3+} and Nd^{3+} ions substitution on structural and magnetic properties of $Co_{0.5}Ni_{0.5}Fe_2O_4$ ferrite system. *Journal of the Indian Chemical Society* **2022**, *99*, 100255, <https://doi.org/10.1016/j.jics.2021.100255>.
42. Suresh Kumar, N.; Padma Suvarna, R.; Chandra Babu Naidu, K. Structural and ferroelectric properties of microwave heated lead cobalt titanate nanoparticles synthesized by sol–gel technique. *Journal of Materials Science: Materials in Electronics* **2018**, *29*, 4738-4742, <https://doi.org/10.1007/s10854-017-8429-6>.